

1 **Specific Codons Control Cellular Resources and Fitness**

2 Aaron M. Love^{a,b}, Nikhil U. Nair^{b,*}

3 ^a Manus Bio, Cambridge, MA 02138

4 ^b Department of Chemical & Biological Engineering, Tufts University, Medford, MA 02155

5 * Corresponding author: nikhil.nair@tufts.edu; @nair_lab

6

7

8 **KEYWORDS:** Codon bias; resource competition; tRNA; protein expression; genetic burden; translation

9

10

11

12

GLOSSARY

- 13 ▪ **RSCU:** Relative synonymous codon usage
- 14 ▪ **W_{ij}:** Relative adaptiveness (weight)
- 15 ▪ **CAI:** Codon adaptation index
- 16 ▪ **ENC:** Effective number of codons
- 17 ▪ **CUB:** Codon usage bias
- 18 ▪ **TAI:** tRNA adaptation index
- 19 ▪ **sTAI:** Species-specific tRNA adaptation index
- 20 ▪ **nTE:** Normalized translational efficiency
- 21 ▪ **RFM:** Ribosome flow model
- 22 ▪ **CFP:** Cyan fluorescent protein
- 23 ▪ **YFP:** Yellow fluorescent protein
- 24 ▪ **TxTL:** in vitro transcription-translation
- 25 ▪ **UTR:** Untranslated region
- 26 ▪ **AUC:** Area under the curve
- 27 ▪ **Fitness:** Performance of induced culture ÷ Performance of uninduced culture
- 28 ▪ **Growth Fitness:** AUC of growth curve (induced) ÷ AUC of growth curve (uninduced)
- 29 ▪ **Co-Expression Fitness:** AUC of YFP fluorescence (with induced CFP or mCherry) ÷ AUC of YFP fluorescence
- 30 (with uninduced CFP or mCherry)
- 31 ▪ **Expression Level:** AUC of fluorescence from induced over-expressed protein (CFP or mCherry)
- 32 ▪ **CHI (χ):** Codon harmony index
- 33 ▪ **MFE:** Mean free energy

34

35

36

37

38

39

40

41

42

43

44 **ABSTRACT:**

45

46 As biotechnology research progresses from simply overexpressing proteins to creating intricate metabolic
47 pathways, gene circuits, and complex phenotypes, harmonizing gene fitness in the context of a host organism has
48 become essential. A significant amount of recent work has focused on decoupling gene expression from host
49 resources to improve the outcome of synthetic biology and metabolic engineering efforts. While insightful, few of
50 these studies have investigated the mechanistic underpinnings of resource allocation during translation
51 elongation. There is a degeneracy in codons – but they are not equivalent. While there is an understanding that
52 codon use is unequal in native genes, there is less knowledge of how this usage bias modulates the supply and
53 demand of protein translation resources. Here we investigate how the partitioning of microbial translational
54 resources, specifically through allocation of tRNA by incorporating dissimilar codon usage bias, can drastically alter
55 expression of proteins and reduce the burden on the host resources. By isolating individual codons experimentally,
56 we find heterologous gene expression can *trans*-regulate fitness of the host and other heterologous genes.
57 Interestingly, specific codons drive profitable or catastrophic phenotypic outcomes. We correlate codon usage
58 patterns with genetic fitness and empirically derive a novel coding scheme for multi-gene expression called Codon
59 Harmony Index (CHI, χ). CHI enables the design of harmonious multi-gene expression systems while avoiding
60 catastrophic cellular burden.

61

62

63 **INTRODUCTION:**

64

65 The genetic code is degenerate with 61 codons and only 20 amino acids, creating an astronomically high level of
66 mRNA sequence space for most protein coding genes. However, it is well accepted that synonymous codons are
67 not equivalent^{1,2}, as numerous reports of *cis* and *trans* effects have been documented³⁻¹¹ – from mRNA structure
68 and co-translational protein folding¹²⁻¹⁴ to tRNA and ribosome competition¹⁵⁻¹⁷. Re-coding proteins typically
69 proceeds through use of a codon adaptation index (CAI), which enables a gene to assume the codon usage bias
70 (CUB) of a reference set, often a set of highly expressed genes¹⁸. This strategy may generally correlate CUB with
71 protein expression, but it ignores the role CUB can play in partitioning translational resources such as tRNA and
72 ribosomes. Several recent studies have demonstrated the ability of heterologous genetic CUB to *trans*-regulate
73 host gene expression through translational resource competition^{19,20}, but there is little understanding of how
74 specific CUB alters host fitness given that cellular resources are invariably limited. Re-coding strategies such as the
75 tRNA adaptation index (tAI)^{7,21} and normalized translational efficiency (nTE)⁶ are attempts to address tRNA related
76 translational supply-demand constraints, but they are limited by how predictive natural CUB and/or tRNA levels
77 are for recombinant protein expression.

78 It is particularly important to consider translational resource competition in the context of multi-gene expression
79 (e.g., in the case of metabolic engineering and synthetic biology), where the objective is often for global organism
80 fitness in addition to high protein expression, and tradeoffs in protein expression can be highly consequential for
81 pathway or genetic circuit function and robustness²². This area is currently underexplored, as most studies to date
82 focus on feedback control mechanisms^{23,24}, resource partitioning^{25,26}, or attempt to draw inferences about
83 elongation in larger genes from libraries limited to the 5' sequence of a reporter^{27,28}, and experiments that do not
84 isolate translation elongation from initiation effects¹⁰. As cellular engineering becomes increasingly complex,
85 genetic resource competition can unravel designs and lead to unpredictable and undesirable phenotypes. While a
86 role for CUB in the partitioning of cellular resources has been reported²⁹, identification of specific codons that
87 present excess translational capacity could provide a novel avenue for harnessing underutilized resources that are
88 insofar ignored.

89 In this study, we systematically isolate the role of codon choices during translational elongation and identify
90 supply-demand constraints imposed on tRNA and ribosomal resources in *E. coli*. We demonstrate that tRNA
91 limitations lead to competition between overexpressed genes as well as with the host's demands. Select codons
92 over-represented in native highly expressed genes are found to cause severe fitness costs when present in
93 overexpressed protein sequences. While the traditional method of codon-optimization through maximizing CAI
94 may promote use of these codons, our data reveal their demand and supply are delicately balanced. We define a
95 new metric called "Codon Harmony Index" (CHI, χ) that quantitatively ranks codons by their capacity to remain
96 orthogonal to host demands. We also posit using this metric as a new codon optimization scheme to mitigate
97 competition with host demands and avoid growth defects. Genes characterized by high scores on this metric
98 scheme demonstrate relatively high expression while minimizing the burden on the host cells, allowing effective
99 multigene expression and cellular growth.

100

101

102 **RESULTS:**

103

104 **Fitness costs are incurred due to translation elongation limitation.**

105

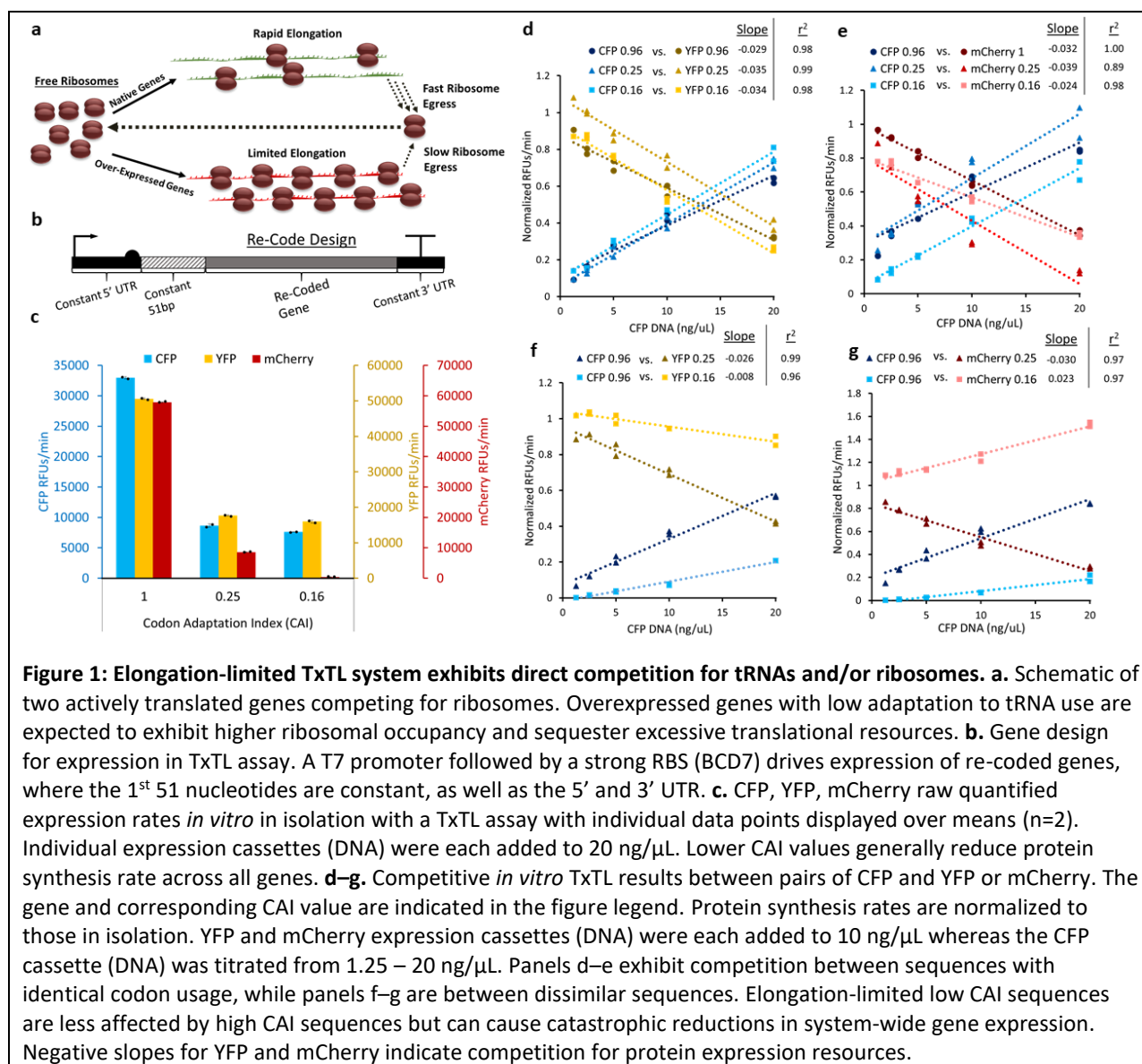
106 Genetic burden is frequently observed in microbial systems as a growth defect upon the overexpression of
107 recombinant proteins²⁴. While the cause of this effect varies, it is often attributed to resource competition at the
108 level of mRNA translation³⁰. In a fast-growing culture of *E. coli*, the availability of free ribosomes can limit mRNA
109 translation, especially in a system with overexpressed protein³¹ (**Figure 1a**). Elongation speed determines the rate
110 at which free ribosomes are made available, hence sub-optimal mRNA transcripts that are poorly translated have
111 higher ribosome occupancy. Such elongation limited mRNA sequences will sequester more ribosomes and return
112 them to the free pool at a slower rate, thus reducing ribosome availability. Translational resource competition has
113 been modeled in several ways³², including the ribosome flow model (RFM)³³, which can be useful in examining
114 translation rate as a function of elongation time that varies depending on the supply and demand of tRNAs in the
115 cell. Applying a previously developed RFM³⁴ to the model gene cyan and yellow fluorescent proteins (CFP and YFP
116 respectively) with high or low CAI values (where CAI is in reference to highly expressed *E. coli* genes) illustrates the
117 increase in mRNA ribosome occupancy that occurs when codons with longer elongation times³⁵ are used, and
118 indicates that elongation-limited sequences are less sensitive to changes in the rate of translation initiation (**Figure**
119 **S1**).

120 We first sought to investigate the impact of translation elongation resource competition using an *in vitro*
121 transcription-translation (TxTL) model. A significant challenge to investigating translational resource competition is
122 the difficulty in isolating any single sequence parameter experimentally, as any synonymous mutation can have a
123 multitude of effects on initiation, elongation, and mRNA structure². A TxTL system allows for better physical
124 control over the genetic expression environment by holding available resources (e.g., ribosomes, tRNAs, aminoacyl
125 tRNA synthetases, RNA polymerase etc.) constant, and allowing precise titration of genes of interest in the
126 reaction. We developed an assay for elongation limitation by leveraging the unique amino acid sequence similarity
127 between CFP and YFP derived from a super-folder green fluorescent protein³⁶, which only differ by 2 amino acids³⁷,
128 thus eliminating variability in protein structure and amino acid demand. The CFP-YFP pair permits the interrogation
129 of competition between various sequence designs using effectively identical proteins, which should also be less
130 susceptible to variation in co-translational protein folding due to their high stability. We also include mCherry in
131 the study, which is <30% identical to CFP-YFP and serves as a comparison point to find trends independent of
132 amino acid sequence (see supplementary data for sequences). The TxTL kit is based off the *E. coli* MRE600 strain,
133 which has a nearly identical CUB as K12 MG1655 and is therefore assumed to be a good proxy for the tRNA profile
134 in a K12 strain used subsequently (**Figure S2**). Reactions were driven by a T7 promoter using a bicistronic domain
135 (BCD) in place of a traditional ribosome binding site to minimize interactions between the 5' untranslated region
136 and gene of interest that could lead to differential expression³⁸. To further isolate translation elongation as the
137 primary variable in sequence design, we chose to keep the 5' and 3' untranslated regions (UTRs) as well as the first
138 51 base pairs (17 codons) constant to mitigate any effect sequence changes may have on translation initiation
139 (**Figure 1b**).

140 Utilizing the idealized TxTL competition assay, we evaluated baseline expression rates from CFP, YFP, and mCherry
141 re-codes with extreme CAI values (0.96, 0.25, or 0.16) (**Figure 1c**). We find that identical sequence pairs for CFP-
142 YFP behave very similarly in terms of relative expression, and that protein expression rates for CFP, YFP, and
143 mCherry correspond well with CAI value. This supports that TxTL recapitulates translation elongation limitation –
144 i.e., genes with lower CAI that use lower abundance tRNAs show lower protein synthesis rates. Next, we examined
145 competition between different pairs of genes. As in the RFM, we expected elongation-limited sequences with
146 lower CAI to disrupt expression of other genes through the sequestration of free ribosomes. We titrated CFP
147 template DNA against constant YFP or mCherry DNA using re-codes with either very high or very low CAI (**Figure**
148 **1d–g**). For instances of two identically re-coded sequences with any CAI tested, YFP and mCherry synthesis rates
149 are inversely correlated with CFP DNA concentration (**Figure 1d–e**), irrespective of their baseline expression,
150 indicating strong competition for limiting resources (i.e., tRNA). This indicates that while an excess protein
151 synthesis capacity exists in the TxTL system, sequences with lower CAI are still resource-limited, likely due to lower
152 availability of tRNA.

153

154



155

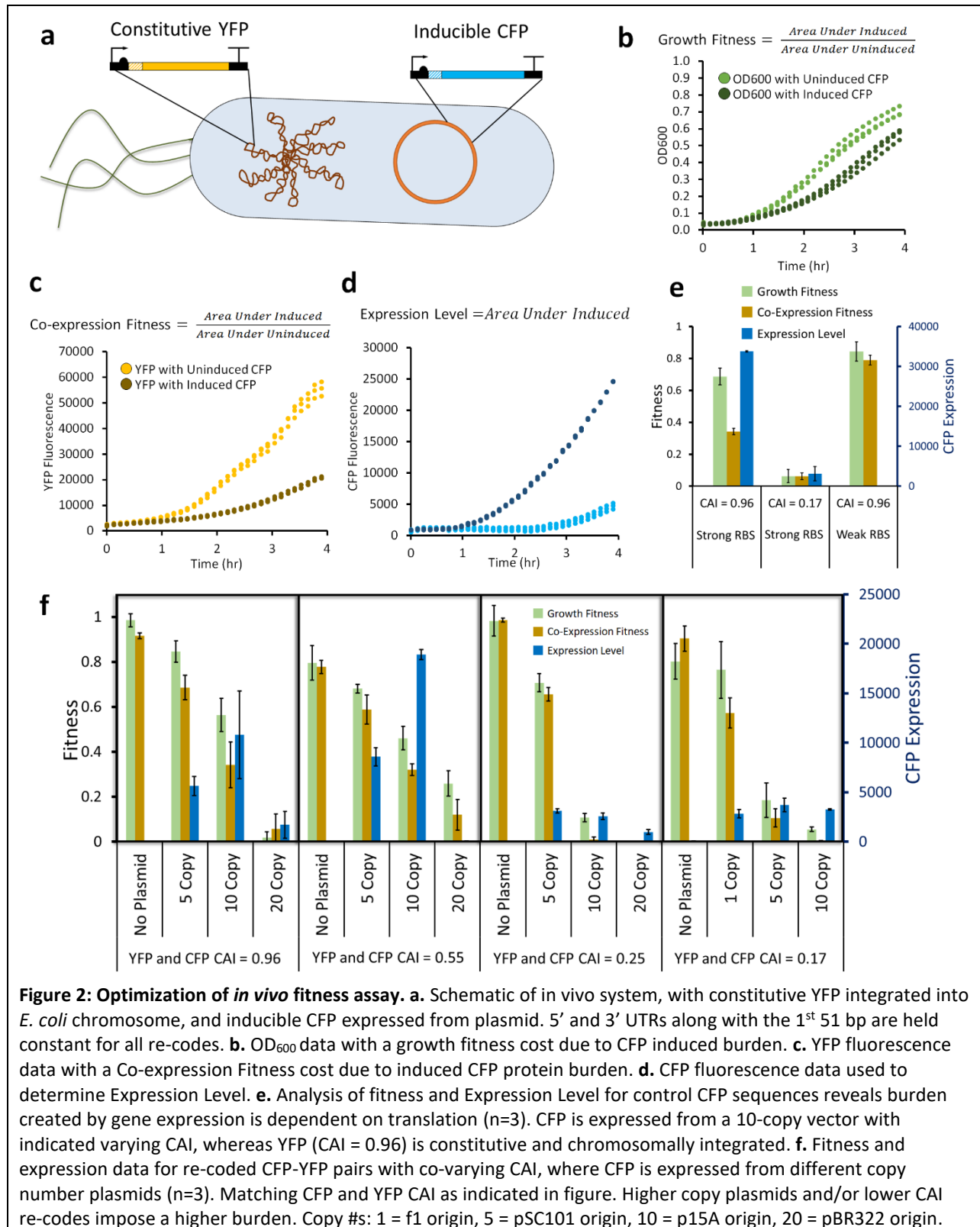
156 **Figure 1: Elongation-limited TxTL system exhibits direct competition for tRNAs and/or ribosomes.** **a.** Schematic of two actively translated genes competing for ribosomes. Overexpressed genes with low adaptation to tRNA use are expected to exhibit higher ribosomal occupancy and sequester excessive translational resources. **b.** Gene design for expression in TxTL assay. A T7 promoter followed by a strong RBS (BCD7) drives expression of re-coded genes, where the 1st 51 nucleotides are constant, as well as the 5' and 3' UTR. **c.** CFP, YFP, mCherry raw quantified expression rates *in vitro* in isolation with a TxTL assay with individual data points displayed over means (n=2). Individual expression cassettes (DNA) were each added to 20 ng/μL. Lower CAI values generally reduce protein synthesis rate across all genes. **d–g.** Competitive *in vitro* TxTL results between pairs of CFP and YFP or mCherry. The gene and corresponding CAI value are indicated in the figure legend. Protein synthesis rates are normalized to those in isolation. YFP and mCherry expression cassettes (DNA) were each added to 10 ng/μL whereas the CFP cassette (DNA) was titrated from 1.25 – 20 ng/μL. Panels d–e exhibit competition between sequences with identical codon usage, while panels f–g are between dissimilar sequences. Elongation-limited low CAI sequences are less affected by high CAI sequences but can cause catastrophic reductions in system-wide gene expression. Negative slopes for YFP and mCherry indicate competition for protein expression resources.

170

171 More interesting observations are seen when dissimilar CAI re-codes are under competition upon co-expression (Figure 1e–f). Low CAI YFP and mCherry synthesis rates are not very sensitive to increasing resource demand by high CAI CFP synthesis. Conversely, the relative CFP expression is much lower than we observed either in isolation or when competing with a high CAI sequence. The observed results appear to be consistent across different sequence pairs, indicating that this phenomenon is independent of protein sequence. When examined in the context of an RFM, we deduce that the rare codon enriched YFP and mCherry sequences sequester ribosomes to such a degree that even excess CFP template DNA does not yield high synthesis rates. On the other hand, YFP and mCherry are not affected due to severe elongation limitation. This model is further supported by our observation that YFP and mCherry rates are reduced when competing with similarly re-coded low CAI CFP sequences, which is a likely consequence of competition for scarce tRNAs. Overall, our data indicates that proteins coded with similar CAI (high or low) are strongly competitive due to demand for the same tRNA pool. Conversely, genes coded under distinct CAI regimes are constrained by the availability free ribosomes, which are in turn limited due to slow/stalled translation from scarce tRNA resources. Our TxTL data strongly support the argument that translation

183

184 elongation limitation could play an important role in cellular resource competition and highlights the impact to
 185 global translational resources (e.g., free ribosomes, tRNA) in multigene expression environments.
 186



187
 188 **Figure 2: Optimization of *in vivo* fitness assay.** **a.** Schematic of *in vivo* system, with constitutive YFP integrated into
 189 *E. coli* chromosome, and inducible CFP expressed from plasmid. 5' and 3' UTRs along with the 1st 51 bp are held
 190 constant for all re-codes. **b.** OD₆₀₀ data with a growth fitness cost due to CFP induced burden. **c.** YFP fluorescence
 191 data with a Co-expression Fitness cost due to induced CFP protein burden. **d.** CFP fluorescence data used to
 192 determine Expression Level. **e.** Analysis of fitness and Expression Level for control CFP sequences reveals burden
 193 created by gene expression is dependent on translation (n=3). CFP is expressed from a 10-copy vector with
 194 indicated varying CAI, whereas YFP (CAI = 0.96) is constitutive and chromosomally integrated. **f.** Fitness and
 195 expression data for re-coded CFP-YFP pairs with co-varying CAI, where CFP is expressed from different copy
 196 number plasmids (n=3). Matching CFP and YFP CAI as indicated in figure. Higher copy plasmids and/or lower CAI
 197 re-codes impose a higher burden. Copy #s: 1 = f1 origin, 5 = pSC101 origin, 10 = p15A origin, 20 = pBR322 origin.

198
199
200
201
202
203
204
205
206
207
208
209
210
211
212
213
214
215
216
217
218
219
220
221
222

We next set out to optimize an in vivo system for *E. coli* expression to efficiently interrogate the effect alternative recoding designs have on gene expression and host fitness. Our system generally consists of a strong constitutively expressed YFP reporter gene (CAI = 0.96) integrated into the *E. coli* chromosome paired with an inducible CFP on a plasmid driven by the inducible promoter P_{trc} with a strong RBS (**Figure 2a**). As before, we held the 1st 51 bases and the 5' and 3' UTRs constant for all re-codes. Cells grown in rich medium with a common pre-culture were passaged under inducing or non-inducing conditions. The area under the curve (AUC) is used to measure each of the 3 signals (growth and 2 fluorescent proteins), which captures the aggregate effects of different lag phases and expression rates (**Figure S3**). We define fitness as the ratio of AUC induced vs. uninduced, which ranges from 0 to 1 for low and high fitness, respectively (or conversely, high and low burden). Fitness can be in terms of Growth Fitness based on OD₆₀₀, or Co-expression Fitness based on YFP fluorescence (chromosomal reporter), while Expression Level is based on CFP or mCherry fluorescence (i.e., the overexpressed protein) (**Figure 2b-d**). We generally observed a reduction in both growth and YFP fluorescence upon CFP induction. Examining several controls expressed from a p15A origin in **Figure 2e**, a “codon-optimized” high CAI CFP gene expresses well but elicits a significant fitness cost in terms of Growth Fitness and Co-expression Fitness. For a CFP recoded with rare codons, the result is catastrophic, and cultures are unable to grow at all. The effect also seems mediated by translation (not transcription) since the codon-optimized CFP with a very weak RBS, but intact promoter neither synthesizes protein nor demonstrates much fitness cost. Upon varying plasmid copy number with several pairs of CFP and YFP with different CAI levels, we found that fitness costs (Co-expression and Growth) were strongly dependent on copy number that is further exacerbated by low CAI (**Figure 2f**). Interestingly, the CFP Expression Level was not very correlated with CAI nor copy number. Based on these results, we picked the 10-copy vector (p15A origin) with the YFP CAI = 0.96 chromosomal reporter as the platform for further studies to investigate recoding schemes that may reduce fitness costs.

223 **Systematic analysis of codon use reveals supply and demand constraints in tRNA resources.**

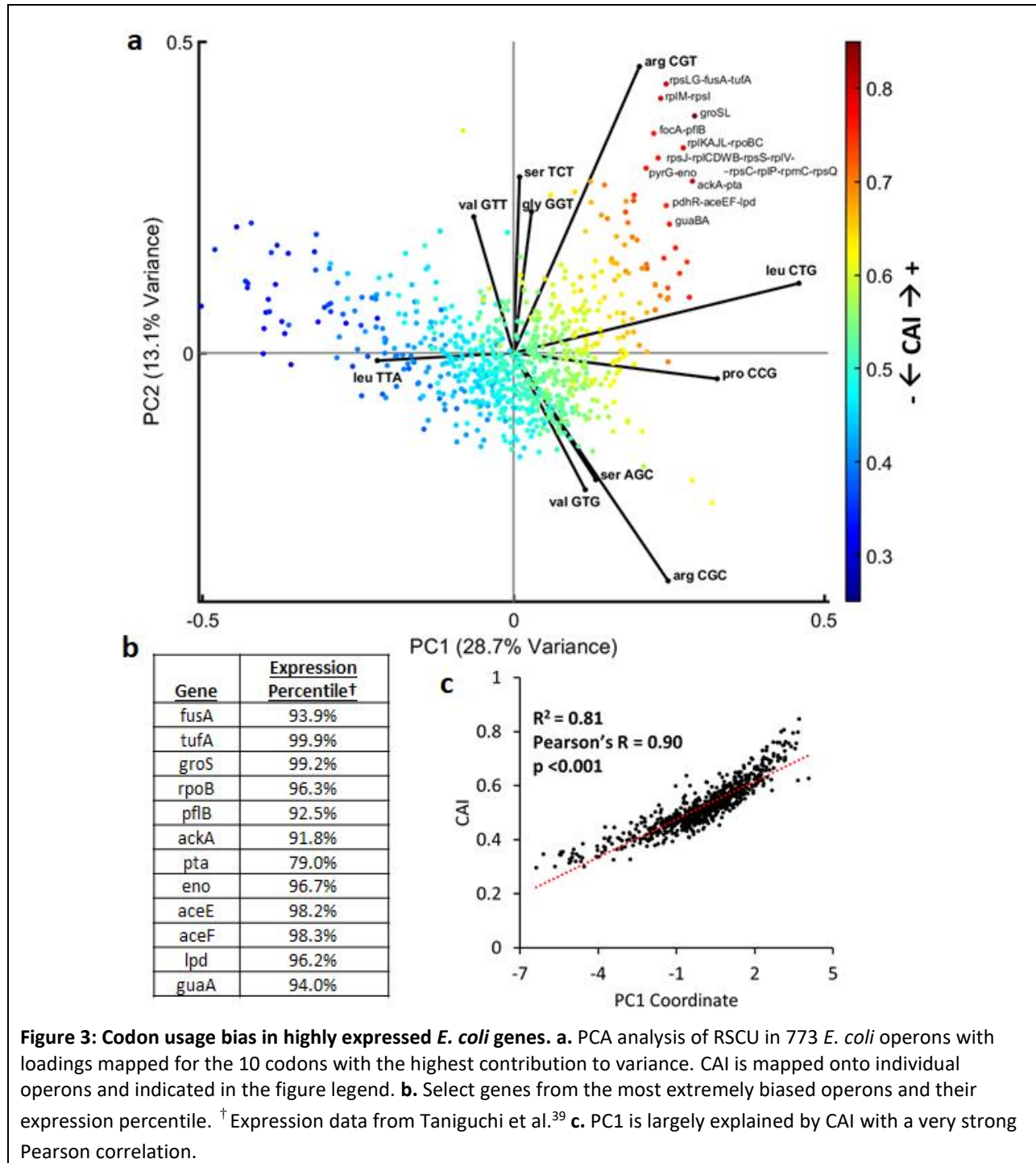
224
225
226
227
228
229
230
231
232
233
234

Prior to designing novel re-coded genes that moderate translation elongation resources, we first investigated CUB in the *E. coli* transcriptome. CAI calculations are typically based on the natural CUB in highly expressed genes. CUB can be represented as a 64-dimensional space (total number of codons) using RSCU values (observed vs. expected frequency) for each protein coding gene. Initial analysis revealed that groups of genes within the *E. coli* transcriptome cluster according to distinct CUB schemes (**Figure S4**). We focused on a consolidated set of this sequence space by analyzing all operons with at least 2 protein coding genes, given that functionally related genes that naturally cluster have similar CUB (**Figure S5**). The resulting 64 dimensions of codon usage across 773 operons can be represented in 2 dimensions accounting for 41.2% of total variance (**Figure S6**) using principal component analysis (PCA) as shown in **Figure 3a**. The loading vectors mapped onto the plot represent the 10 codons that contribute most significantly to codon bias across the 773 operons.

235
236
237
238
239
240
241
242
243
244
245
246
247
248

This analysis captures the CUB naturally observed in the *E. coli* transcriptome and highlights a positive correlation between CAI and expression. This is expected because here CAI is calculated by optimizing towards CUB in highly expressed genes¹⁸ (see methods) (**Figure S7**). Consistent with previous studies, we corroborate that genes in the most extremely biased CUB space are some of the most highly expressed genes in the *E. coli* proteome that often serve essential functions (**Figure 3b**). The natural bias leading to the CAI scale is very well explained by PC1 (**Figure 3c**). Despite the apparent correlation between CAI and expression, studies have reported that CAI often does not predict higher gene expression¹⁰. Importantly, the CAI paradigm of re-coding proteins to match the CUB of highly expressed genes ignores potential resource competition that can occur at the tRNA level. For 18 of 20 amino acids, multiple codons exist, and 10 of 18 of those can be coded to use different tRNAs in *E. coli* K12 MG1655 (**Figure S8**). Upon examining the PCA loadings, there are clearly particular codons that are very overrepresented in highly expressed proteins (e.g., arg CGT, leu CTG, and pro CCG). For such high-demand codons, using alternative codon/tRNA pairs, or even codons that recruit tRNAs with weaker affinity, have the potential to reduce translation elongation-based resource competition between overexpressed proteins and native essential and/or highly expressed genes.

249



250

251

252

253

254

255

256

257

258

259

260

261

262

Using our optimized in vivo assay, we sought to experimentally determine the contribution of individual codons to gene Expression Level and Co-Expression Fitness. The synonymous codon sequence space that could be explored in even a small gene such as CFP is experimentally intractable. Holding the first 51 bp constant and co-varying all possible synonymous codons would produce a massive library size of 1.8×10^{104} . While a more constrained codon library is possible, we chose a focused experimental approach by interrogating individual codon contribution to

263 gene Expression Level and Co-Expression Fitness. Starting with a CFP or mCherry sequence having a high CAI (0.96
264 – 1.0) and using a single codon for each amino acid where the effective number of codons (ENC) = 20 (for details
265 on ENC, see methods), for each amino acid we re-coded every instance to another synonymous codon, resulting in
266 a total of 41 possible re-coded sequences (= 64 possible codons – 20 high CAI codons already in use – 3 stop
267 codons) (**Figure 4a**). Results were normalized in terms of both Expression Level and Co-expression Fitness (defined
268 in **Figure 2b**) relative to the high CAI parent control (**Figure 4b**) and indicate wide ranging benefits or costs. In
269 several instances, alternative codons provide a significant improvement in Co-Expression Fitness across both
270 mCherry and CFP. Variations in phenotypes could in part be due to different amino acid composition between
271 mCherry and CFP, as the number of re-coded amino acids was not held constant between genes (**Figure S9**). We
272 chose to re-code all instances of each amino acid so as not to limit the number of altered codons to the amino acid
273 with the fewest instances. Most of the re-codes do not improve expression (**Figure 4c**), which is expected since
274 they were derived from (and normalized to) high CAI sequences that emulate highly expressed genes. CFP and
275 mCherry re-codes are also less consistent in Expression Level than Co-Expression Fitness, reflecting a higher degree
276 of variability between genes in *cis* compared *trans* effects. Notably, there are several alternative codons for
277 leucine, proline, and one for arginine, which robustly improve Co-expression Fitness, suggesting that dissimilar
278 codon use could be a means to generally reducing heterologous gene burden. Expression Level and Co-expression
279 Fitness do not correlate well for mCherry or CFP re-codes (**Figure 4d–e**), indicating that while there may be general
280 tradeoffs between expression and fitness, there are many instances where specific codon/tRNA pairs possess
281 excess translational capacity.

282
283

284 **Novel recoding scheme yields genes with robustly improved fitness.**

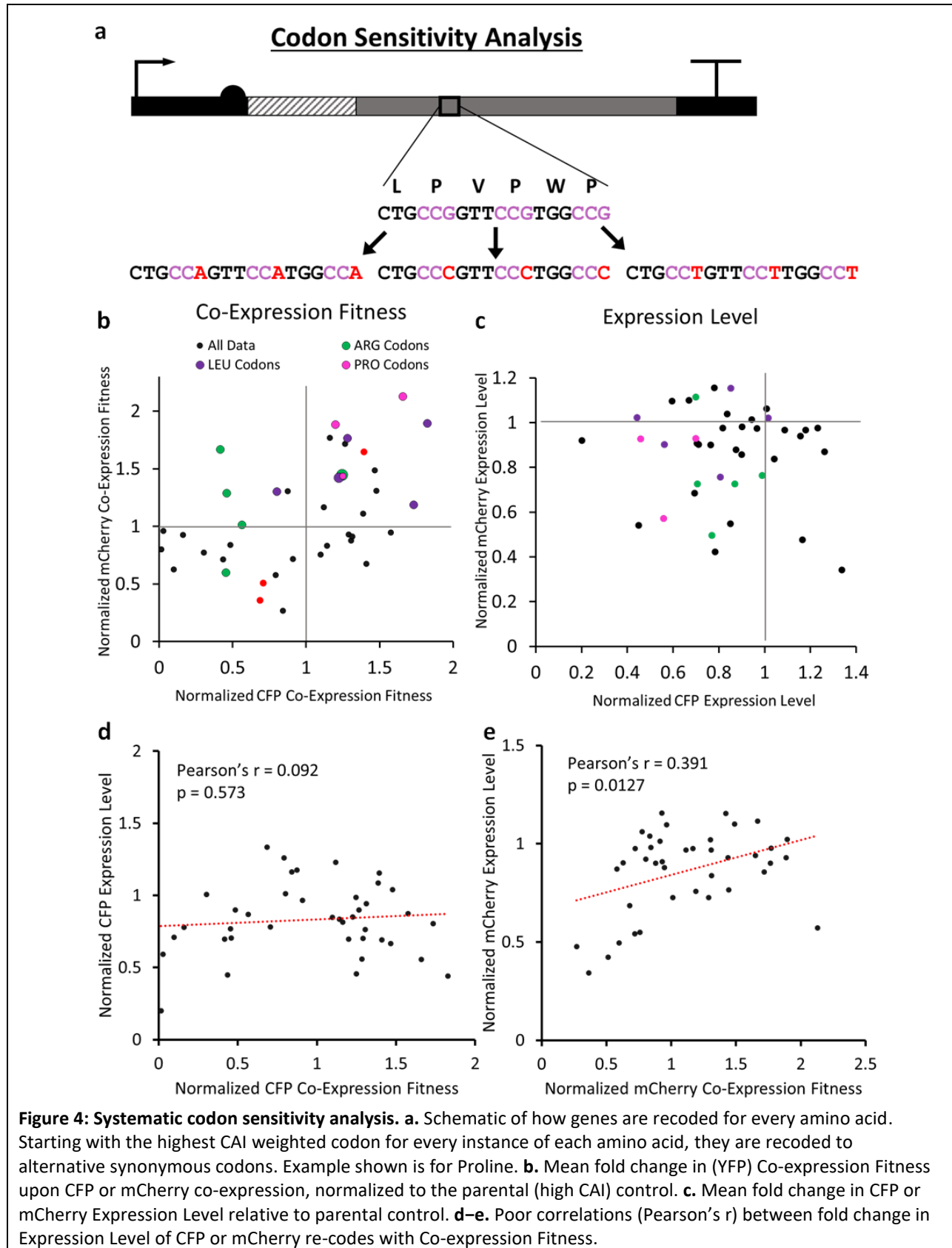
285

286 Next, we developed a new recoding index derived from Co-expression Fitness values for individual codons in
287 **Figure 4b**. We chose to focus on fitness rather than expression since our primary aim was to investigate how re-
288 coding schemes can modulate resource competition during translation elongation. To convert the Co-expression
289 Fitness data for CFP and mCherry re-codes into generalized codon weights, we took the Euclidean distance from
290 the origin to the coordinates of each data point shown in **Figure 4b** as a raw score for each sequence, where each
291 parent codon held a normalized coordinate value of (1,1). Similar to calculating CAI, relative adaptiveness (W_i)
292 scores were then determined by normalizing the raw weights from each amino acid codon set to the codon with
293 the highest fitness (see methods and **Data S1**). We refer to this new metric as the Codon Harmony Index (CHI or χ).

294

295 A comparative analysis between CUB in the overall *E. coli* genome, CAI (using highly expressed genes as a
296 reference), and χ reveals that χ favors very different codon use than CAI and discourages use of codons enriched in
297 highly expressed genes (**Figure 5a**), notably for Arg CGT, Leu CTG, and Pro CCG. There are instances where χ and
298 CAI do correspond well (e.g., Gly GGA, GGC, GGG), but many codons show inverse trends between the two scales.
299 Generally, amino acids with multiple available tRNAs (including Arg, Leu, and Pro) correspond with larger
300 differences between expected RSCU values calculated for CAI and χ (and shown in **Figure 5a**), suggesting that
301 recruitment of different tRNAs is playing a role in determining Co-Expression Fitness (**Figure S10**). Interestingly, χ
302 favored codons do not always correspond to amino acids with multiple available tRNAs, indicating tRNA
303 abundance may not alone account for the observed effect, which could also be in part due to different translation
304 efficiencies created by favorable interactions of tRNA codon-anticodon pairs.

305



306
 307
 308
 309
 310
 311
 312
 313

314 Utilizing the new χ weights, we next created several CFP and mCherry sequences that were optimized to varying
315 degrees on the new χ scale (**Figure 5b**). Specifically, we created a $\chi = 1$, ENC = 20 sequence, along with 4 sets of 3
316 different sequences each holding χ constant at 0.95, 0.85, 0.75, and 0.65 for both CFP and mCherry by using a
317 greedy algorithm (**Figure S11**). The lower end of the χ scale for the CFP/mCherry genes was approximately 0.6,
318 which is dictated by the protein sequence, and lowest W_{ij} values for each set of codons (see methods). Thus, the
319 effective working range of χ is $\sim 0.6 - 1.0$ compared to CAI that operates from $\sim 0.2 - 1.0$. When the χ recoded
320 sequences were assayed for fitness and expression (**Figure 5c-e**), there was a very strong positive correlation
321 between CFP and mCherry analogous re-codes for fitness and expression, indicating that these synonymous coding
322 schemes are a primary determinant for how a gene performs regardless of amino acid sequence. Remarkably, we
323 also observe a strong positive correlation between χ and, both, Growth Fitness and Co-Expression Fitness—
324 indicating that the weights derived from the individual codon assay are additive to improve the fitness of various
325 globally-recoded sequences (**Figure S12**). High χ sequences clearly provide reduced competition for host resources
326 and improved fitness. The χ scale is less predictive of expression, which is expected as it was not part of the criteria
327 used to create the codon weights. Despite this, there is a good correlation between CFP and mCherry re-coded
328 sequences in terms of Expression Level, indicating that codon usage bias does generally predict expression.
329 Importantly, there are several sequences with reduced burden that retain relatively high expression, which
330 represents an excess translational capacity for sequences re-coded using high χ values.
331

332 To investigate which codon usage bias patterns have the greatest contribution to Co-expression Fitness, we
333 analyzed RSCU across all variable 59 codon dimensions (excluding stop, Trp, and Met codons) for each of the CFP
334 and mCherry re-coded sequences (as seen in **Figure 5b**) using PCA (**Figure 6**). We were able to represent 46.7% of
335 the total sequence variation in the first 3 dimensions (**Figure S13**) when analyzing the CFP and mCherry re-codes'
336 RSCU along with 773 *E. coli* operons. Here again PC1 and PC2 primarily explain variation across *E. coli* sequences,
337 but intriguingly we see a new highly orthogonal dimension in PC3 that explains variation in the χ sequences, and
338 PC1 vs. PC3 best differentiate the χ re-coded sequences from natural *E. coli* operons. The χ sequences generally
339 have intermediate to low values on the CAI scale with low overall CAI variation, meaning they would not have been
340 predicted to express well using CAI (**Figure 6a**). This is somewhat surprising given that many of the re-codes with
341 moderate to high χ (0.8–0.95) still exhibit relatively high expression compared with the high CAI control as
342 demonstrated in **Figure 5e**. When mapping χ values to the data, we see that χ describes variation along PC3 very
343 well (**Figure 6b, Figure S14**). *E. coli* operon sequences do not vary significantly on the χ scale, implying that the re-
344 coded sequences explore novel coding schemes orthogonal to natural sequence space. Examining the loadings for
345 the 3 most biased natural codons, we find that the high χ sequences are using synonymous variations for Arg, Leu,
346 and Pro that differ as expected from highly expressed genes. We conclude that competition for tRNA isoacceptors
347 in high demand by highly expressed essential genes primarily drives competition for translation elongation
348 resources and avoiding specific codons that are over-represented in such native genes provides a novel strategy to
349 improve the Co-Expression Fitness of heterologous genes.
350

351 Given the breadth of existing knowledge regarding codon optimization, we also evaluated how χ compares with
352 other reported CUB strategies such as the tRNA adaptation index (tAI)⁷ and normalized translation efficiency
353 (nTE)⁶. These approaches weight codons based on their co-adaptation to the tRNA pool or the tRNA supply vs.
354 codon demand respectively. We calculated the expected RSCU of a perfectly adapted gene sequence using these
355 various scales to assess their degree of similarity (**Figure S15**), and found that stAI (species specific TAI using *E. coli*
356 specific weights)²¹ correlates the closest with χ (Pearson's $r = 0.393$, $p = 0.002$), but does not provide as much
357 differentiation between codons available for each amino acid. We suspect the primary differentiator of the χ re-
358 coding strategy relative to tAI or nTE is that it provides empirical insight into which specific codons have excess
359 capacity for translation as opposed to an approach relying solely on genomic statistics and approximations. Further
360 analysis of the χ re-coded sequences did not reveal any consistent correlation with secondary structure or GC
361 content between CFP and mCherry re-codes, supporting the notion that specific codon use is likely driving
362 sequence behavior (**Figure S16**). We also re-coded 10 random genes with 3 free commercial re-coding algorithms
363 to analyze whether any of them exhibit exploration of χ related CUB strategies and found that they generally vary
364 along classical *E. coli* CUB and seek to adapt to host codon use without optimizing in the χ sequence space (**Figure**
365 **S17**).

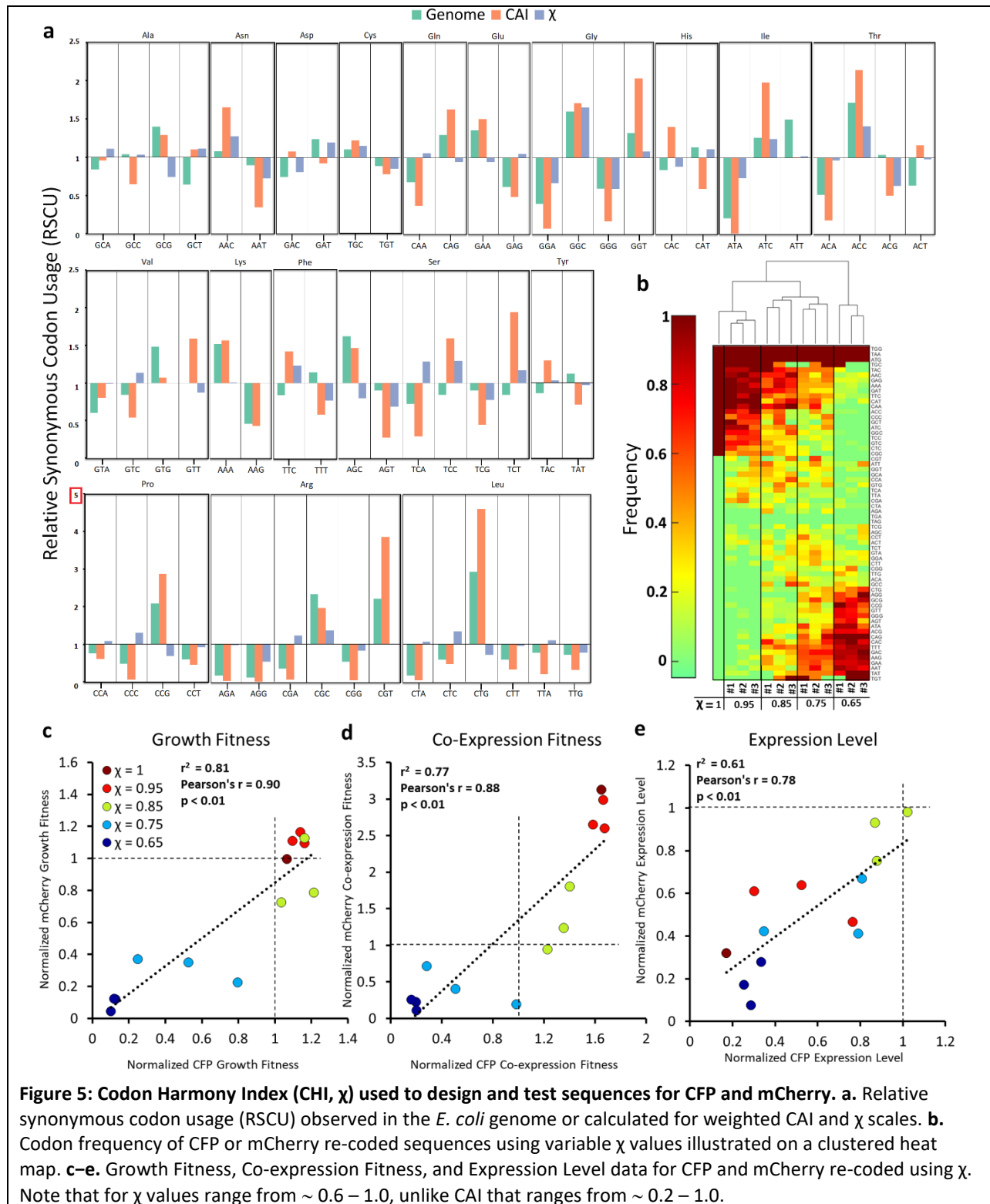
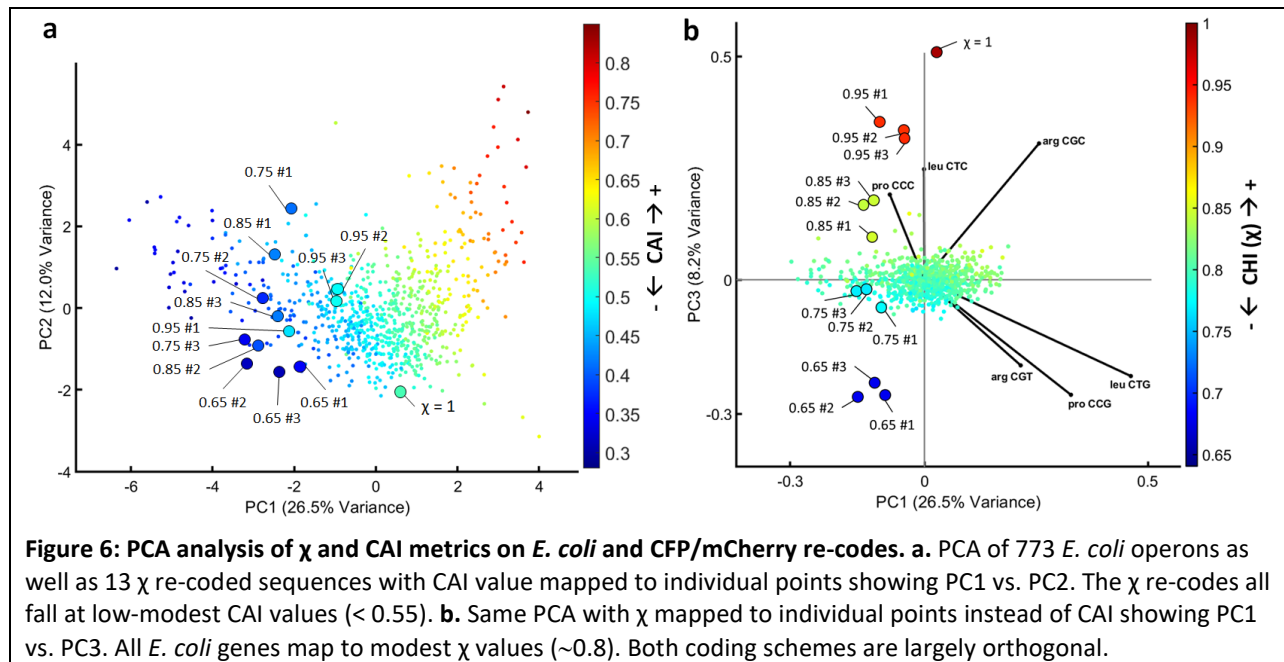


Figure 5: Codon Harmony Index (CHI, χ) used to design and test sequences for CFP and mCherry. a. Relative synonymous codon usage (RSCU) observed in the *E. coli* genome or calculated for weighted CAI and χ scales. **b.** Codon frequency of CFP or mCherry re-coded sequences using variable χ values illustrated on a clustered heatmap. **c–e.** Growth Fitness, Co-expression Fitness, and Expression Level data for CFP and mCherry re-coded using χ . Note that for χ values range from $\sim 0.6 - 1.0$, unlike CAI that ranges from $\sim 0.2 - 1.0$.

366
367
368
369
370
371
372
373

374 In theory, χ could also correlate with CUB in phages that infect *E. coli* and have co-adapted to maximize gene
375 expression without overwhelming host resources. There have been reports of not only co-adaptation to tRNA
376 pools^{40,41}, but also translational selection for CUB dissimilarity between viruses and hosts to avoid excessive

377 competition for tRNAs⁴². We examined codon usage in 12 common coliphages known to infect *E. coli* to examine
378 whether CUB in such parasitic viruses may have evolved to harmonize with bacterial hosts as a means to allow
379 better co-utilization of shared translational resources (**Figure S18**). Our analysis indicates that phage genes
380 generally tend to avoid CUB at high values of CAI (> 0.7) and exhibit a slightly higher mean χ than *E. coli* genes. This
381 suggests that it may be more productive in the phage life cycle to avoid excessive similarity and competition with
382 their host, but there is another unique aspect of the CUB in χ that was not strongly selected for in phages. It is
383 possible that the translational resource demand from an overexpressed protein on a multi-copy vector is higher
384 than natural genes have encountered and is thus under a higher level of translational selection resulting in novel
385 types of advantageous CUB reflected by χ that cannot be inferred from natural sequence space.
386



387
388 **Figure 6: PCA analysis of χ and CAI metrics on *E. coli* and CFP/mCherry re-codes. a.** PCA of 773 *E. coli* operons as
389 well as 13 χ re-coded sequences with CAI value mapped to individual points showing PC1 vs. PC2. The χ re-codes all
390 fall at low-moderate CAI values (< 0.55). **b.** Same PCA with χ mapped to individual points instead of CAI showing PC1
391 vs. PC3. All *E. coli* genes map to moderate χ values (~0.8). Both coding schemes are largely orthogonal.

392

393

394 DISCUSSION:

395

396 Protein translation is one of the most resource intensive cellular processes, which has yielded significant CUB
397 observed in nature, especially in single cellular microorganisms often used as expression hosts⁴³. Most
398 conventional codon optimization strategies operate under the key assumption that translational selection in
399 naturally evolved systems provides CUB that is relevant for the overexpression of heterologous genes. This may be
400 partially true, but realistically, the overexpression of genes can push host resource demand beyond levels required
401 for native gene expression⁴⁴, resulting in translational selective pressures that organisms haven't evolved with.
402 Protein expression must also be considered in the context of increasingly complicated engineered systems, and
403 often in synthetic biology and metabolic engineering efforts, overexpression is not nearly as important as reliable
404 and predictable gene expression and host fitness⁴⁵. Here we have revealed both in vitro and in an *E. coli* model
405 that translation elongation can limit protein expression, and often has profitable or catastrophic consequences on
406 system-wide resource availability.

407 In our TxTL assay, we found that proteins coded with similar CAI compete for the same tRNA supply, and re-coded
408 genes can reduce such competition. Consequently, high CAI sequences are ribosome-limited, demonstrating
409 reduced synthesis rates that are also highly sensitive to competition. In certain cases, low CAI genes are
410 monopolistic or anti-competitive with free ribosomes and are thus insensitive to increased demand from high CAI
411 sequences, albeit at the expense of overall resources. Theoretical frameworks have been well established to
412 explain how resource limited translation can lead to the sequestration of ribosomes, but these studies generally

413 rely on ribosome footprinting data³⁵ and tRNA copy number^{6,7} to infer codon elongation times, which are indirect
414 measurements of ribosome flux on a given mRNA.

415 Our novel experimental approach using an *E. coli* model demonstrates the sensitivity of system resources at
416 individual codon resolution and reveals key differences between the optimal CUB for highly expressed native genes
417 vs. overexpressed proteins. Several previous studies have investigated CUB using randomized libraries that fail to
418 thoroughly explore the vast sequence space available when re-coding a gene⁴⁶. Such randomized sequences will
419 generally regress to intermediate RSCU values for each codon, and rarely sample the extremities of the sequence
420 space available (**Figure S19**). By systematically re-coding individual amino acids to each alternate codon in multiple
421 proteins, we have methodically investigated how individual codons contribute to gene Expression Level and Co-
422 Expression Fitness at further extremities of the theoretical design space than have been previously explored. The
423 avoidance of codons with very high CUB in native essential genes (e.g., for Arg/Leu/Pro) is a novel driver of
424 reduced genetic burden.

425 We used individual codon sensitivity data to create a new re-coding strategy that optimizes for fitness (CHI or χ)
426 and demonstrate how the new codon weighting method enables the creation of unique CUB strategies that are
427 not represented naturally in *E. coli*. Using PCA for dimensional reduction, our methodology reveals how sequences
428 with identical CAI scores can still exhibit distinct variations in CUB that result in different phenotypes, namely
429 improvements in Co-Expression Fitness. Remarkably, globally re-coded sequences were found to have predictable
430 phenotypes informed from the additive effects of individual codon use, allowing us to leverage a relatively small
431 dataset to predict phenotypes in a vast sequence space. While global sequence characteristics including GC
432 content, structure, and a variety of sequence motifs are all known to contribute to protein expression², our results
433 suggest that codon bias is a strong predictor of both protein expression and fitness and can be optimized
434 independently of the UTRs or 5' coding sequence. An analysis of *E. coli* phage CUB reveals that while parasitic
435 organisms may avoid over-use of preferred host codons, a concept that has been recently suggested⁴², the
436 demands of heterologous gene over-expression and resulting selective pressures are likely to have different
437 resource demands than those of viruses, and thus may have overlapping yet still largely distinct CUB fitness
438 landscapes.

439
440 The data-informed strategy in this study represents an approach that could be extended to other microbes
441 including eukaryotic systems, where ongoing controversy over the impact CUB has on host-gene fitness has been
442 unresolved⁴⁷⁻⁵¹. While our study included 2 proteins (CFP and mCherry) with very different amino acid sequences,
443 measuring Expression Level and Co-Expression Fitness for additional proteins could further refine χ , and provide
444 additional insight for maximizing expression and fitness together. The new χ metric is more predictive of *trans*
445 effects (Co-expression Fitness) than *cis* effects (Expression Level), thus further optimization of translation initiation
446 and CUB that maximizes both expression and fitness is an interesting future objective. The observation that there
447 are several sequences with relatively high expression and high fitness illustrates there are solutions to co-optimize
448 both genetic traits. In practice, re-coding genes with high CAI will often lead to higher expression with low overall
449 fitness, but re-coding with high χ values (between 0.9-0.95) should provide reasonably high expression with more
450 orthogonal resource demands. Similar data sets could also be collected for any organism where protein expression
451 is feasible, which could also provide insights into how species differ in the role CUB plays regarding resource
452 allocation. It is possible that with more inter-species data, organism specific χ weights could be predicted *a priori*
453 based on the avoidance of codons overrepresented in host genes. Practically, this study should improve the
454 predictability and robustness of genetic engineering by enabling the co-optimization of gene expression and
455 fitness, especially for multi-gene expression systems.

456

457 **MATERIALS AND METHODS:**

458

459 **Equations used to assess codon usage bias.**

460 We calculated codon adaptation following the classical method reported originally by Sharp and Li¹⁸. This method
461 relies on first calculating relative synonymous codon usage (**RSCU**) in a genetic sequence, which is defined by

462 **Equation 1:**

$$RSCU_{ij} = \frac{X_{ij}}{\frac{1}{n_i} \sum_{j=1}^{n_i} X_{ij}} \quad (1)$$

463 RSCU calculates the observed frequency of codon **j** belonging to amino acid **i** divided by expected frequency,
464 where **X** is the number of occurrences for codon **j** in a given sequence. The expected frequency is simply the
465 number of occurrences for any codon belonging to amino acid **i**, divided by the number of codons (**n**) available for
466 that particular amino acid. RSCU is used instead of raw frequency values to normalize observed codon frequency
467 based on the total codons available. An RSCU value < 1 indicates bias against the codon, while an RSCU value > 1
468 indicates a bias toward the codon, and RSCU = 1 indicates no bias. The RSCU values for each codon can be used to
469 calculate relative adaptiveness (**W**), which is defined by **Equation 2:**

$$W_{ij} = RSCU_{ij} / RSCU_{imax} \quad (2)$$

470 Relative adaptiveness is the RSCU for a codon **j** belonging to amino acid **i** divided by the RSCU for the codon in the
471 set for amino acid **i** with the highest RSCU value (*imax*). In other words, **W** gives a value of 1 for codons in a target
472 sequence that match the frequency of the most common codon in a reference sequence. **W** values are used in
473 calculating the codon adaptation index (**CAI**) defined by **Equation 3:**

$$CAI = \left(\prod_{k=1}^L w_k \right)^{1/L} \quad (3)$$

474

475 CAI is the geometric mean of the **W** values for each codon in a given sequence containing **L** codons. Importantly,
476 the reference sequence(s) and calculated RSCU values that **W** values are derived from can be from any source.
477 Unless otherwise indicated, in this study, CAI refers to **W** values for a set of highly expressed set of *E. coli* genes.
478 Alternatively, CAI can be computed based on **W** values for CUB across the entire genome, sTAI weights²¹, or χ
479 weights (**See Data S2 for W values used in various calculations**). Normalized translational efficiency (nTE) was
480 calculated as previously described⁶ by taking the ratio of species specific TAI weights for *E. coli*²¹ (supply) vs. the
481 codon use across the *E. coli* transcriptome (demand) defined by **Equation 4:**

$$nTE_{ij} = sTAI_{ij} / Frequency_{ij} \quad (4)$$

482 The nTE_{ij} values are analogous to W_{ij} values for the calculation of nTE, which proceeds the same as for CAI by taking
483 the geometric mean across a sequence (as in equation 3). In this study, nTE was calculated using genomic codon
484 frequency as opposed to codon use (originally defined as codon occurrence multiplied by RNA transcript
485 abundance), as the two were found to be highly correlated (**Figure S20**). Lastly, the effective number of codons
486 (**ENC**) is often used as a measure of codon bias in a sequence, and is calculated using **Equation 5:**

$$ENC = 2 + \frac{9}{F_2} + \frac{1}{F_3} + \frac{5}{F_4} + \frac{3}{F_6} \quad (5)$$

487

488 ENC can take a value from 20, in the case of extreme bias where one codon is exclusively used for each amino acid,
489 to 61 when the use of alternative synonymous codons is equally likely. The value F is the average probability that
490 two randomly selected codons for an amino acid with n number of synonymous codons will be identical⁵².

491

492 **Data sources used in analysis.**

493 Genomic codon usage for *E. coli* K12 MG1655 and *E. coli* MRE600 were assessed by analyzing codon bias from
494 published annotated genomes obtained from NCBI under the accession numbers NC_000913.3 and CP014197.1
495 respectively using MATLAB. Phage analysis was done with annotated phage genomes from NCBI, and accession
496 numbers are listed in **Figure S18**. Exact codon frequencies and relative adaptiveness values (W) used in this study
497 for calculating CAI in reference to highly expressed genes CUB, entire genome CUB, sTAI, or nTE, can be found in
498 **Data S2**. The W values for χ and associated information from the study can be found in **Data S1**. W values for
499 highly expressed genes were originally downloaded online from GenScript, and were cross referenced to published
500 values⁵³. The sTAI codon weights were downloaded online from a publically available database ([http://tau-
501 tai.azurewebsites.net/](http://tau-tai.azurewebsites.net/))²¹. The tRNA copy numbers referenced in this study (**Figure S8**) were downloaded from the
502 Genomic tRNA Database (<http://gtrnadb.ucsc.edu/>)⁵⁴.

503

504 **Ribosome flow model.**

505 The implemented ribosome flow model (RFM) (**Figure S1**) was adapted from Zur et al. using open source Matlab®
506 code³⁴. In this model, an mRNA is divided into n number of chunks, where each chunk is 9 codons (27 bases),
507 approximately the footprint of an *E. coli* ribosome. Translation time of each chunk is based on local λ , which is a
508 sum of the individual times it takes to translate each codon in a chunk. Codon times used are available in **Data S3**.
509 Ribosome collisions are also accounted for in the model as a function of the ribosome density in adjacent
510 positions. In this model, the protein production rate is the rate of translation of the final position on the mRNA.
511 For this application, steady state ribosome densities were computed for CFP and YFP re-coded to use preferred
512 (high CAI) or rare (low CAI) codons. To demonstrate the relationship between initiation rate and translation rate
513 for different sequences, steady state protein production rates are calculated for different initiation rates.

514

515 **Gene design and re-coding.**

516 All genetic re-coding designs and analysis were executed in Matlab® using custom functions. Code is made
517 available online at <https://github.com/nair-lab>. A full list of amino acid and DNA sequences used in this study can
518 be found in **Data S4**. CFP and YFP were initially cloned through site directed mutagenesis of an existing super-
519 folder GFP protein based on previously reported sequences.^{37,55} For the systematic analysis of codon use design,
520 CFP or mCherry were re-coded starting from highly biased sequences using the most preferred codon for each
521 amino acid (CAI = 1 and ENC = 20), not taking into account the first 17 codons. The first 17 codons were held
522 constant for all re-codes and were based on previously used sequences that functionally expressed well. A Matlab®
523 script was then used to systematically design sequences where every instance of an amino acid was mutated to a
524 single alternate synonymous codon. In the design of sequences with novel re-coding schemes, a greedy algorithm
525 was used (**Figure S11**), that functions by randomly mutating a codon to a synonymous alternative, then evaluating
526 whether the new sequence is closer to the target CAI (or in this specific instance χ value). To re-code CFP and
527 mCherry to a desired χ value, a starting sequence was first randomized to ensure there was no initial bias, and then
528 the algorithm was followed to the target χ value. We generated several unique output sequences with the same χ
529 value but different coding sequences, then selected 3 sequences for each value of χ tested making sure they were
530 substantially different from each other based on hierarchal clustering done in Matlab®.

531

532 **Plasmids and strain construction.**

533 All plasmids were cloned from existing vectors with restriction enzyme sites already present (**figure S21, S23, Data**
534 **S4**), which also contained 5' and 3' UTRs. Genes were all custom ordered synthesized as full length double

535 stranded DNA fragments with AarI restriction sites on the 5' and 3' termini. A type IIS restriction enzyme cloning
536 approach with AarI was used to insert synthesized double stranded DNA gene fragments into the desired vector.
537 All constructs were sequence verified from clonally pure DNA using Sanger sequencing across the gene and UTRs.
538 The screening strain used to assess Co-Expression fitness was engineered from *E. coli* K12 MG1655 (CGSC#: 6300).
539 The YFP reporter was integrated in an intergenic region (~3,938,000 bp) between the *rsmG-atpI* genes using λ -
540 Red based homologous recombination of the YFP CAI = 0.96 sequence, which was under the control of a strong
541 constitutive promoter (FAB46) and RBS (BCD7) based on a previous study,³⁸ and a 5' insulator and 3' terminator
542 (**Figure S22, Data S4**). The method of integration and marker excision method has been previously reported
543 (Datsenko and Wanner).⁵⁶ Briefly, a linear cassette consisting of the gene, UTRs, and an attached kanamycin
544 resistance marker was amplified by PCR with ~500bp of homology to the desired locus on either end.
545 Chromosomally integrated clones were identified by colony PCR and sequence verified via Sanger sequencing of
546 the PCR product including several hundred bases of chromosomal DNA and the entire integrated heterologous
547 expression cassette. Sequence verified clones had the integrated kanamycin marker removed through the
548 previously described FLP-FRT site specific recombinase method and were again Sanger sequenced for final
549 verification.

550

551 **in vitro transcription-translation (TxTL) assay.**

552 The TxTL assay was carried out using the NEB PURExpress® kit (E6800). This assay relies on T7 polymerase, and
553 consists of purified reconstituted components. Accordingly, CFP, YFP, and mCherry expression cassettes were first
554 cloned into a pBAC vector with a T7 promoter and strong RBS (BCD7) (**Figure S23 a–b, Data S4**). The genes were
555 also flanked by an insulator and terminator sequence on the 5' and 3' UTR respectively. Once clonally pure and
556 sequence verified, expression cassettes were amplified by PCR (from the beginning of the insulator to end of the
557 terminator) and normalized in concentration using UV-vis spectroscopy at $\lambda = 260\text{nm}$. A master mix was first
558 prepared according to the PURExpress® published protocol, which was kept on ice until use. Reactions were scaled
559 down to 5 μL final volume and carried out in Corning® low volume 384-well white flat bottom polystyrene TC-
560 treated microplates (part # 3826). Reactions were initiated by the addition of DNA using a multi-channel pipette
561 ($n=2$ per condition), followed by immediate transfer to a Tecan Infinite® M1000 microplate reader. A DNA
562 concentration of 20ng/ μL each was found to generally maximize competition between two genetic cassettes
563 (**Figure S23 c-d**). Assays were run for 6hr. at 37°C with fluorescent reads every 5 minutes of each protein being
564 analyzed (CFP: Ex. 435nm, Em. 470nm, YFP: Ex. 510nm, Em. 530nm, mCherry: Ex. 585nm, Em. 612nm). Reported
565 reaction rates reflect the maximum rate observed.

566

567 **in vivo fitness and expression assay.**

568 To assess Co-Expression Fitness, Growth Fitness, and Expression Level, sequence verified plasmid constructs were
569 transformed into *E. coli* K12 MG1655 with the chromosomally integrated YFP reporter. Unless noted otherwise,
570 overexpressed proteins were under control of the Trc promoter with a strong RBS (BCD7) (**Data S4**). 3 individual
571 transformants were isolated and grown overnight in 400 μL LB broth (BD Difco™) with selective antibiotic at 37°C in
572 96 deep well plates (Greiner Bio-One MASTERBLOCK®, 96 Well, 2 ML Item: 780270) for 24 hr. Cultures were then
573 split and diluted 1:40 into LB broth with selective antibiotic and with or without 500 μM inducer (IPTG) in black 96
574 well clear bottom micro-titer plates (Thermo product: 165305). Plates were incubated for 8 hours with shaking at
575 37°C in a Tecan Infinite® M1000 microplate reader with monitoring every 5 minutes for OD600, as well as
576 fluorescence (CFP: Ex. 435nm, Em. 470nm, YFP: Ex. 510nm, Em. 530nm, mCherry: Ex. 585nm, Em. 612nm). Data
577 were analyzed by comparing induced vs. uninduced cultures in terms of fluorescence and growth. To account for
578 lag phase and differences in rates within a single term, the background subtracted area under the curve (AUC) was
579 used for each respective signal using a Matlab® numerical integrator. The timespan evaluated was bounded by the
580 time it took any sample to reach the upper limit of detection for fluorescence, which often took between 4-6
581 hours.

582

583

584 **Additional data analysis.**

585 Linear regression, correlation analysis, dimensional reduction, and associated statistics were calculating using built
586 in functions in Matlab[®]. Principal component analysis and hierarchal clustering were always carried out on an m x
587 n matrix of RSCU values with codons in 61 rows and n number of gene sequences in columns. For RNA folding
588 calculations, the minimum free energy was calculated for sequences using the Vienna RNAfold Version 2.5.1
589 software.⁵⁷

590

591 **COMPETING INTERESTS:**

592 The authors declare no competing or conflicting interests.

593

594

595 **ACKNOWLEDGMENT AND FUNDING:**

596 ManusBio supported and funded this work. We thank members of the Nair lab for thoughtful discussions and
597 advice.

598

599

600 **ASSOCIATED CONTENT:**

601 There are 24 figures included in the Supplemental Information, and there are 4 supplementary data files.

602

603

604 **DATA AVAILABILITY STATEMENT:**

605 Additional data are available upon request. Additional supplementary Matlab[®] code can be found at
606 <https://github.com/nair-lab/CHI>.

607

608

609 **AUTHOR CONTRIBUTIONS:**

610 A.M.L. performed the experimental work and data analysis. A.M.L. and N.U.N. conceived the study, planned the
611 experiments, and wrote/edited the manuscript.

612

613

614

615 **REFERENCES:**

616

- 617 1. Plotkin, J. B. & Kudla, G. Synonymous but not the same: the causes and consequences of codon bias. *Nat. Rev. Genet.* **12**, 32–42 (2011).
- 618
- 619 2. Quax, T. E. F., Claassens, N. J., Söll, D. & van der Oost, J. Codon Bias as a Means to Fine-Tune Gene Expression. *Mol. Cell* **59**, 149–161 (2015).
- 620
- 621 3. Frumkin, I. *et al.* Gene Architectures that Minimize Cost of Gene Expression. *Mol. Cell* **65**, 142–153 (2017).
- 622 4. Ikemura, T. Correlation between the abundance of Escherichia coli transfer RNAs and the occurrence of the
- 623 respective codons in its protein genes: A proposal for a synonymous codon choice that is optimal for the E.
- 624 coli translational system. *J. Mol. Biol.* **151**, 389–409 (1981).
- 625 5. Boël, G. *et al.* Codon influence on protein expression in E. coli correlates with mRNA levels. *Nature* **529**,
- 626 358–363 (2016).
- 627 6. Pechmann, S. & Frydman, J. Evolutionary conservation of codon optimality reveals hidden signatures of
- 628 cotranslational folding. *Nat. Struct. Mol. Biol.* **20**, 237–243 (2013).
- 629 7. Reis, M. d., Savva, R. & Wernisch, L. Solving the riddle of codon usage preferences: a test for translational
- 630 selection. *Nucleic Acids Res.* **32**, 5036–5044 (2004).
- 631 8. Tuller, T. *et al.* An Evolutionarily Conserved Mechanism for Controlling the Efficiency of Protein Translation.
- 632 *Cell* **141**, 344–354 (2010).
- 633 9. Goodman, D. B., Church, G. M. & Kosuri, S. Causes and Effects of N-Terminal Codon Bias in Bacterial Genes.
- 634 *Science (80-.)*. **342**, 475–479 (2013).
- 635 10. Kudla, G., Murray, A. W., Tollervey, D. & Plotkin, J. B. Coding-Sequence Determinants of Gene Expression in
- 636 Escherichia coli. *Science (80-.)*. **324**, 255–258 (2009).
- 637 11. Presnyak, V. *et al.* Codon optimality is a major determinant of mRNA stability. *Cell* **160**, 1111–1124 (2015).
- 638 12. Saunders, R. & Deane, C. M. Synonymous codon usage influences the local protein structure observed.
- 639 *Nucleic Acids Res.* **38**, 6719–6728 (2010).
- 640 13. Ciryam, P., Morimoto, R. I., Vendruscolo, M., Dobson, C. M. & O’Brien, E. P. In vivo translation rates can
- 641 substantially delay the cotranslational folding of the Escherichia coli cytosolic proteome. *Proc. Natl. Acad.*
- 642 *Sci.* **110**, E132–E140 (2013).
- 643 14. Yu, C.-H. *et al.* Codon Usage Influences the Local Rate of Translation Elongation to Regulate Co-
- 644 translational Protein Folding. *Mol. Cell* **59**, 744–754 (2015).
- 645 15. Kafri, M., Metzl-Raz, E., Jona, G. & Barkai, N. The Cost of Protein Production. *Cell Rep.* **14**, 22–31 (2016).
- 646 16. Borkowski, O. *et al.* Cell-free prediction of protein expression costs for growing cells. *Nat. Commun.* **9**, 1457
- 647 (2018).
- 648 17. Dong, H., Nilsson, L. & Kurland, C. G. Co-variation of tRNA Abundance and Codon Usage in Escherichia coli at
- 649 Different Growth Rates. *J. Mol. Biol.* **260**, 649–663 (1996).
- 650 18. Sharp, P. M. & Li, W. The codon adaptation index—a measure of directional synonymous codon usage bias,
- 651 and its potential applications. *Nucleic Acids Res.* **15**, 1281–1295 (1987).
- 652 19. Lipinszki, Z. *et al.* Enhancing the Translational Capacity of E. coli by Resolving the Codon Bias. *ACS Synth.*
- 653 *Biol.* **7**, 2656–2664 (2018).
- 654 20. Lyu, X., Yang, Q., Zhao, F. & Liu, Y. Codon usage and protein length-dependent feedback from translation
- 655 elongation regulates translation initiation and elongation speed. *Nucleic Acids Res.* **49**, 9404–9423 (2021).
- 656 21. Sabi, R., Volvovitch Daniel, R. & Tuller, T. stAI calc : tRNA adaptation index calculator based on species-

- 657 specific weights. *Bioinformatics* **33**, btw647 (2016).
- 658 22. Boo, A., Ellis, T. & Stan, G. B. Host-aware synthetic biology. *Curr. Opin. Syst. Biol.* **14**, 66–72 (2019).
- 659 23. Shopera, T., He, L., Oyetunde, T., Tang, Y. J. & Moon, T. S. Decoupling Resource-Coupled Gene Expression in
660 Living Cells. *ACS Synth. Biol.* **6**, 1596–1604 (2017).
- 661 24. Ceroni, F. *et al.* Burden-driven feedback control of gene expression. *Nat. Methods* **15**, 387–393 (2018).
- 662 25. Huang, H.-H., Qian, Y. & Del Vecchio, D. A quasi-integral controller for adaptation of genetic modules to
663 variable ribosome demand. *Nat. Commun.* **9**, 5415 (2018).
- 664 26. Darlington, A. P. S., Kim, J., Jiménez, J. I. & Bates, D. G. Dynamic allocation of orthogonal ribosomes
665 facilitates uncoupling of co-expressed genes. *Nat. Commun.* **9**, 695 (2018).
- 666 27. Frumkin, I. *et al.* Gene Architectures that Minimize Cost of Gene Expression. *Mol. Cell* **65**, 142–153 (2017).
- 667 28. Cambray, G., Guimaraes, J. C. & Arkin, A. P. Evaluation of 244,000 synthetic sequences reveals design
668 principles to optimize translation in *Escherichia coli*. *Nat. Biotechnol.* **36**, 1005–1015 (2018).
- 669 29. Frumkin, I. *et al.* Codon usage of highly expressed genes affects proteome-wide translation efficiency. *Proc.*
670 *Natl. Acad. Sci.* **115**, E4940–E4949 (2018).
- 671 30. Nieß, A., Siemann-Herzberg, M. & Takors, R. Protein production in *Escherichia coli* is guided by the trade-
672 off between intracellular substrate availability and energy cost. *Microb. Cell Fact.* **18**, 8 (2019).
- 673 31. Vind, J., Sørensen, M. A., Rasmussen, M. D. & Pedersen, S. Synthesis of Proteins in *Escherichia coli* is
674 Limited by the Concentration of Free Ribosomes. *Journal of Molecular Biology* vol. 231 678–688 (1993).
- 675 32. Gorochowski, T. E., Avcilar-Kucukgoze, I., Bovenberg, R. A. L., Roubos, J. A. & Ignatova, Z. A Minimal Model
676 of Ribosome Allocation Dynamics Captures Trade-offs in Expression between Endogenous and Synthetic
677 Genes. *ACS Synth. Biol.* **5**, 710–720 (2016).
- 678 33. Reuveni, S., Meilijson, I., Kupiec, M., Ruppín, E. & Tuller, T. Genome-Scale Analysis of Translation
679 Elongation with a Ribosome Flow Model. *PLoS Comput. Biol.* **7**, e1002127 (2011).
- 680 34. Zur, H., Cohen-Kupiec, R., Vinokour, S. & Tuller, T. Algorithms for ribosome traffic engineering and their
681 potential in improving host cells' titer and growth rate. *Sci. Rep.* **10**, 21202 (2020).
- 682 35. Dana, A. & Tuller, T. The effect of tRNA levels on decoding times of mRNA codons. *Nucleic Acids Res.* **42**,
683 9171–9181 (2014).
- 684 36. Pédelacq, J.-D., Cabantous, S., Tran, T., Terwilliger, T. C. & Waldo, G. S. Engineering and characterization of
685 a superfolder green fluorescent protein. *Nat. Biotechnol.* **24**, 79–88 (2006).
- 686 37. Day, R. N. & Davidson, M. W. The fluorescent protein palette: tools for cellular imaging. *Chem. Soc. Rev.* **38**,
687 2887 (2009).
- 688 38. Mutalik, V. K. *et al.* Precise and reliable gene expression via standard transcription and translation initiation
689 elements. *Nat. Methods* **10**, 354–360 (2013).
- 690 39. Taniguchi, Y. *et al.* Quantifying *E. coli* Proteome and Transcriptome with Single-Molecule Sensitivity in
691 Single Cells. *Science (80-.)*. **329**, 533–538 (2010).
- 692 40. Chithambaram, S., Prabhakaran, R. & Xia, X. The Effect of Mutation and Selection on Codon Adaptation in
693 *Escherichia coli* Bacteriophage. *Genetics* **197**, 301–315 (2014).
- 694 41. Lucks, J. B., Nelson, D. R., Kudla, G. R. & Plotkin, J. B. Genome Landscapes and Bacteriophage Codon Usage.
695 *PLoS Comput. Biol.* **4**, e1000001 (2008).
- 696 42. Chen, F. *et al.* Dissimilation of synonymous codon usage bias in virus–host coevolution due to translational
697 selection. *Nat. Ecol. Evol.* **4**, 589–600 (2020).
- 698 43. Nieß, A., Siemann-Herzberg, M. & Takors, R. Protein production in *Escherichia coli* is guided by the trade-

- 699 off between intracellular substrate availability and energy cost. *Microb. Cell Fact.* **18**, 8 (2019).
- 700 44. Ceroni, F., Algar, R., Stan, G.-B. & Ellis, T. Quantifying cellular capacity identifies gene expression designs
701 with reduced burden. *Nat. Methods* **12**, 415–418 (2015).
- 702 45. McBride, C. D., Grunberg, T. W. & Del Vecchio, D. Design of genetic circuits that are robust to resource
703 competition. *Curr. Opin. Syst. Biol.* **28**, 100357 (2021).
- 704 46. Schmitz, A. & Zhang, F. Massively parallel gene expression variation measurement of a synonymous codon
705 library. *BMC Genomics* **22**, 149 (2021).
- 706 47. Shen, X., Song, S., Li, C. & Zhang, J. Synonymous mutations in representative yeast genes are mostly
707 strongly non-neutral. *Nature* **606**, 725–731 (2022).
- 708 48. Rodríguez-Beltrán, J. *et al.* Translational demand is not a major source of plasmid-associated fitness costs.
709 *Philos. Trans. R. Soc. B Biol. Sci.* **377**, (2022).
- 710 49. Torrent, M., Chalancon, G., De Groot, N. S., Wuster, A. & Madan Babu, M. Cells alter their tRNA abundance
711 to selectively regulate protein synthesis during stress conditions. *Sci. Signal.* **11**, 1–10 (2018).
- 712 50. Zhou, Z. *et al.* Codon usage is an important determinant of gene expression levels largely through its
713 effects on transcription. *Proc. Natl. Acad. Sci.* **113**, E6117–E6125 (2016).
- 714 51. Xia, X. A Major Controversy in Codon-Anticodon Adaptation Resolved by a New Codon Usage Index.
715 *Genetics* **199**, 573–579 (2015).
- 716 52. Wright, F. The ‘effective number of codons’ used in a gene. *Gene* **87**, 23–29 (1990).
- 717 53. Taniguchi, Y. *et al.* Quantifying E. coli Proteome and Transcriptome with Single-Molecule Sensitivity in
718 Single Cells. *Science (80-.)*. **329**, 533–538 (2010).
- 719 54. Chan, P. P. & Lowe, T. M. GtRNADB 2.0: an expanded database of transfer RNA genes identified in
720 complete and draft genomes. *Nucleic Acids Res.* **44**, D184–D189 (2016).
- 721 55. Pédelacq, J.-D., Cabantous, S., Tran, T., Terwilliger, T. C. & Waldo, G. S. SI_Engineering and characterization
722 of a superfolder green fluorescent protein. SF DsRed FR FR FR FR DsRed. *Nat. Biotechnol.* **37** (2006).
- 723 56. Datsenko, K. A. & Wanner, B. L. One-step inactivation of chromosomal genes in Escherichia coli K-12 using
724 PCR products. *Proc. Natl. Acad. Sci.* **97**, 6640–6645 (2000).
- 725 57. Lorenz, R. *et al.* ViennaRNA Package 2.0. *Algorithms Mol. Biol.* **6**, 26 (2011).
- 726
- 727